This is a preprint, the final version is subject to change, of the American Mineralogist (MSA)
Cite as Authors (Year) Title. American Mineralogist, in press.
(DOI will not work until issue is live.) DOI: http://dx.doi.org/10.2138/am-2017-6270

Revision 2

A Novel Carbon Bonding Environment in Deep Mantle High-Pressure Dolomite

C. E. Vennari,[1]* Q. Williams[1]

[1]Department of Earth and Planetary Sciences, University of California Santa Cruz, CA 95064

Abstract

The main source of carbon entering the deep Earth is through subduction of carbonates, including $CaMg(CO_3)_2$-dolomite. We examine the high-pressure structure and stability of dolomite to understand the means through which carbon can be sequestered as it enters the deep Earth carbon cycle. Dolomite is investigated to 86 GPa using Raman spectroscopy at room temperature: this includes spectroscopic characterization of dolomite-III, a phase stable at deep mantle pressures and temperatures. Between 63-86 GPa, within the dolomite-III structure, we observe spectroscopic evidence for the evolution of a subpopulation of carbonate ions characterized by *weaker* C-O bonds, with anomalous pressure shifts: this abnormal bonding change is explained by the onset of a 3+1 coordination of the carbon in some of the carbonate ions in the dolomite-III structure, confirming an earlier prediction of Merlini et al. (2012). The wide suite of carbonate ions (both normal 3-fold and 3+1 coordinate) within this phase at the highest pressures should give rise to a large variety of cation sites: as such, dolomite-III could represent a major host for incompatible elements in the deep mantle, implying that incompatible element distribution may be closely linked to carbon cycling within the deep Earth.

Keywords: dolomite, high pressure, Raman spectroscopy, carbon, distorted cation sites, deep Earth

Introduction

Carbonate minerals have long been accepted as the primary carriers of carbon into the deep Earth. Carbonates are present in and on oceanic plates, and when slabs are subducted, oxidized carbon is brought into the deep Earth (e.g., Alt and Teagle 1999). Carbon can have a strong influence on the chemical and physical properties of the mantle (Duba and Shankland 1982; Dasgupta et al. 2006; Shcheka et al. 2006), so its manner of retention at depth is critical for clarifying its role in deep Earth geophysical and petrologic processes. In higher temperature slabs, carbonates likely decompose and release CO_2, which facilitates melting in the Earth's deep upper mantle (e.g., Rosenthal et al. 2015), and can explain carbon dioxide's ubiquity in back arc volcanoes. However, in high pressure and temperature experiments that mimic cold slab geotherms, carbonate and peridotite phase equilibria indicate that carbonate minerals could persist at least down to the transition zone, and possibly deeper (e.g., Litasov et al. 2013). Moreover, primordial carbon could also be retained within Earth's deep mantle, in addition to recycled carbon from subduction (e.g., Hirschmann and Dasgupta 2009).

Dolomite ($CaMg(CO_3)_2$) is a common carbonate on the surface of the earth, is found in sedimentary environments and vein deposits, and crystallizes with rhombohedral symmetry in the space group R-3. There have been several previous high pressure experiments on dolomite at room temperature (300 K). Using spectroscopic and X-ray diffraction (XRD) methodology, two well defined transitions of dolomite to dolomite-II and dolomite-III have been identified around 15-20 GPa and 36-38 GPa, respectively (Santillán et al. 2003; Santillán and Williams 2004; Mao et al. 2011; Merlini et al. 2012; Efthimiopoulos et al. 2017). Merlini et al. (2012), using single crystal X-ray diffraction reported a triclinic, calcite-II-like structure for dolomite-II above 17 GPa and a larger triclinic, calcite-III unit cell for dolomite-III above 35 GPa. Most importantly, Merlini et al. (2012) heated their samples to 2200 K at up to 72 GPa, and Mao et al. (2011) to

~1500 K to 83 GPa, and their results demonstrate that dolomite-III is stable at these extreme conditions. Hence, dolomite-III represents a likely carbon repository at the conditions of Earth's lower mantle. The dolomite-III structure reported by Merlini et al. (2012) is structurally novel, as extrapolated trends of their refinements of interatomic distances to 60 GPa indicate that some of the carbonate ions could adopt a 3+1 coordination with the oxygens at pressures of 60-80 GPa. Experimental and theoretical evidence for the presence of 4-fold coordinate carbon in oxides at high pressures have been previously described (Isshiki et al. 2004; Oganov et al. 2006; Sun et al. 2009; Boulard et al. 2011, 2015; Cerantola et al. 2017; Merlini et al. 2017).

Here, we utilize vibrational spectroscopy to probe the local bonding environment of the carbonate ion (and Ca/Mg cations) within dolomite to 86 GPa: a substantially higher pressure range than previous vibrational studies, and nearly 50 GPa higher than where a previous study (Efthimiopoulos et al. 2017) was unable to resolve any Raman bands from dolomite. Our goals are to evaluate whether dolomite-III undergoes the predicted continuous transition to partial 3+1 coordination of carbon, and to probe the character of the bonding environment of the carbon ion within dolomite-III at these extreme conditions.

Experimental Methods

Dolomite, $Ca_{1.00}Mg_{0.92}Fe_{0.08}(CO_3)_2$, from New Almaden, CA (UCSC mineral collection no. 7206) was used for this experiment: this composition was confirmed using a JEOL JXA-8230 electron microprobe. The sample identity was confirmed using Raman spectroscopy and single crystal XRD, and our results are in excellent agreement with previous studies of nearly endmember dolomite (for example, Nicola et al. 1976). The samples were single crystals with approximate dimensions of 20x20x10 μm. High pressures were generated with a symmetric-type Princeton type diamond anvil cell equipped with type Ia diamonds with 250 μm culets.

Neon was used for the pressure medium, and ruby fluorescence was used as the in-situ pressure calibrant (Mao et al. 1986).

Raman measurements were performed using a Horiba LabRAM HR Evolution spectrometer. Both 532 and 633 nm excitation lasers were used for different regions of the spectrum: 532 nm was used to collect spectra from ~1,400 to 1,800 cm^{-1}, and 633 nm was used for 50-1,325 cm^{-1}. The spectrometer focal length was 800 mm, and it was equipped with a 1,200 lines/mm grating, and a CCD detector. Spectral resolution was ~1 cm^{-1}, and spectra were collected from 1-2 micron spots. Spectra were analyzed and peaks deconvolved with a combination of Lorentzian and Gaussian peaks using Horiba Labspec6 software.

Room pressure single crystal analysis was collected at the Advanced Light Source (beamline 11.3.1). Diffraction images were collected with a Bruker D8 diffractometer with a photon 100 SiMOS detector at 298 K. The single crystal sample characterized was a clear cube that was free of visible cracks and/or imperfections. The sample was mounted in oil on a MiTeGen MicroMount. Images were collected using Bruker APEX II software and integrated using the program SAINT.

Results and Discussion

Our lower pressure (up to 38 GPa) Raman results (Figs. 1 and 2, Table S1 and S2) are consistent with previous work (Mao et al. 2011; Merlini et al. 2012; Efthimiopoulos et al. 2017) in that we observe two discontinuous, first-order transitions: one at ~15 GPa and another at ~40 GPa respectively. Factor group analysis of the optic modes of dolomite-I, with the space group R-3 (Steinfink and Sans 1959), yields $\Gamma = 4A_g$ (R) + $4E_g$ (R) + $5A_u$ (IR) + $5E_u$ (IR). Dolomite-II, with space group P-1 (Merlini et al. 2012), yields $\Gamma = 30A_g$ (R) + 27 A_u (IR). Factor group analysis on dolomite-III, with space group P-1 (Merlini et al. 2012), yields $\Gamma = 120A_g$ (R) and 117 A_u

(IR). Previous studies on different starting materials report the transitions to high-pressure phases of dolomite at modestly higher and lower pressures, respectively (Table S3). Results on decompression are not reported; our highest pressure run reconverted to dolomite-I on decompression, with all modes returning to their initial values, with a possible strain-enhanced mode present at 225 cm^{-1}: this involves an increase in amplitude of a weak Raman active mode, with A_g symmetry (Pilati et al. 1998).

Dolomite-III: Lattice modes at high pressure

Above 42 GPa, at least 11 discrete low-frequency vibrational modes can be resolved in the ~200-600 cm^{-1} range, implying that a broad suite of divalent cation environments and divalent ion/carbonate vibrational interactions are present within the dolomite-III high-pressure phase (Fig. 1, 2b, Table S4). In short, a broad continuum of bands is present, implying that a range of environments is present, consistent with the low symmetry of the dolomite-III structure: this diversity of environments appears to be enhanced above 60-70 GPa, as new bands appear near 450 and 660 cm^{-1}, at the lower frequency and higher frequency sides of this manifold.

From a mantle geochemical standpoint, our observation of the markedly enhanced breadth spanned by the low frequency bands (Fig. 1) is consistent with dolomite-III having a broad suite of distorted cation environments. This conclusion is consistent with the lower pressure crystal structure results of Merlini et al. (2012), and the suggestion that these distortions are notably enhanced at pressures above 63 GPa. Hence, given both the thermal stability of dolomite-III at these pressures (Mao et al. 2011) and that the major phases comprising the deep mantle have highly symmetric cation sites (e.g. Wicks and Duffy 2016), the prospect exists that the irregular cation sites in dolomite-III could represent a major depository for highly incompatible elements in the deep mantle. In particular, the highly irregular 6-11 coordinated

115 cation sites whose bond distances and angles vary significantly in this phase (Table S5) may
116 represent a primary locus in which rare earths could undergo defect substitutions, similar to those
117 present in calcium perovskites (Corgne and Wood 2005). In this sense, the dolomite-III phase in
118 the deep Earth could mimic the geochemical affinities for incompatible elements of carbonatite
119 melts at shallower depths.

120 **Dolomite-III: Carbonate modes at high pressure**

121 The Raman-active carbonate modes provide bonding environment information at high
122 pressures, including constraining the bonding changes taking place within and dolomite-III under
123 compression. At the higher pressures probed, our results support an increase in coordination
124 number of a subset of the carbonate ions. At 41 GPa, the out-of-plane and in-plane bends
125 broaden and approach each other in frequency; by 50 GPa, the two types of vibrations merge into
126 a multiplet of energetically similar modes (~9) which span 140 cm^{-1} in width. This coalescence
127 is generated by the small (or negative) pressure shifts of the out-of-plane bends coupled with the
128 positive shifts and increases in width of the in-plane bends. Near 58 GPa, the highest frequency
129 band in this multiplet disappears, and at 68 GPa, a new low frequency band appears near 750 cm^{-1}
130 , and becomes progressively more intense up to the maximum pressure of 86 GPa (Fig. 1, 2a,
131 Table S4).

132 This appearance of a new lower frequency mode, and disappearance of the highest
133 frequency mode, within the in-plane and out-of-plane bending set of bands, implies that the force
134 constants associated with some O-C-O linkages in the crystal have weakened. This wide breadth
135 of the bending vibrational levels is likely driven by extremely distorted carbonate ions, with both
136 angle variations between the oxygen atoms and the planarity of the ions being variable. The
137 progressive increase in the bending vibrations with pressure in dolomite-III indicates that

repulsive forces with neighboring oxygens may play a larger role than cation-oxygen interactions with the carbonate unit.

The behavior of the symmetric stretch provides further confirmation that a subset of the C-O bonds in dolomite-III weakens at the higher pressures of our study. At the onset of the dolomite-III transition, the single strong peak splits into 5-6 separate components at 41 GPa (Fig. 1, 2a, Table S4), with pressure shifts in accord with those of symmetric stretches in a wide range of carbonates (e.g., Kraft et al. 1991; Gillet et al. 1993; Koch-Müller et al. 2016; Efthimiopoulos et al. 2017). At 64 GPa, two low intensity peaks on the low frequency side of the symmetric stretch emerge from this multiplet. These low-frequency peaks shift at essentially negligible rates between 64 and 86 GPa (Fig. 1 (inset), 2a, Table S4).

As with the in-plane and out-of-plane bends, these new stretching bands at lower frequency than the main group of peaks show that the C-O bonds within a subset of the carbonate ions within the unit cell are dramatically weakened. These bands are anomalous in terms of both their lower frequency (which is consistent with a ~12% decrease in C-O force constant relative to the frequency of the centroid of the symmetric stretching bands), and their negligible pressure shifts (which imply that the force constants of the C-O bonds associated with these vibrations do not increase as the crystal is compacted: this lack of a positive shift, despite compaction, is consistent with a progressive pressure-induced weakening of this subset of C-O bonds).

3+1 Coordination of the carbonate ion

We attribute these new carbonate bands and their associated mode shifts to a less tightly bound carbon configuration, which we attribute to the 3+1 coordination of carbon (Fig. 1c) predicted by Merlini et al. (2012). In the dolomite-III structure proposed by Merlini et al. (2012),

there are eight crystallographically distinct carbon sites within the unit cell; we observe six symmetric stretching peaks after deconvolution, in which some vibrations of carbonate ions may be energetically indistinguishable. Merlini et al. (2012) extrapolated their single crystal data and speculated that an uncommon 3+1 coordination of one of the carbonate ions in the unit cell would ultimately arise, with the planar carbonate ion approaching tetrahedral coordination around 80-90 GPa. In the highest pressure (56 GPa) structure reported by Merlini et al. (2012) the carbonate ion containing the C1 atom is notably distorted (Table S5) in terms of its angular variance from 120˚ and its torsion angle. This distortion is likely a response to the close approach of its nearest-neighboring, non-bonded oxygen atom, O12. The interatomic distance between C1 and O12 is 2.066 Å at 56 GPa, and strongly decreases with pressure. The C1 carbonate ion the most likely to undergo a coordination change to 3+1 coordination; the carbonate ion that is bonded to O12 is also likely to approach 3+1 coordination. This C7-associated carbonate ion is the most distorted with respect to its angle variance, with O-C-O angles that range from 108˚ to 133˚ with an angle variance of 12.6˚ (Table S6). Our Raman spectra appear to record the onset of higher coordination (and hence weaker C-O bonding) through both the appearance of the lowest frequency symmetric stretch peak that appears above 63 GPa, and the onset of a low frequency bend vibration, and disappearance of the highest frequency component of the bends.

The lowest frequency mode associated with the carbonate symmetric stretch at 63 GPa compared to the median of the symmetric stretching band is ~12%. this amount approaches the difference between those observed between XY_3 and XY_4 molecular species with the same cations and anions (e.g. boron halides) (Nakamoto 1986). Thus, a partial coordination change involving a progressively increasing interaction with an approaching oxygen anion explains both

the decreased frequency of these new bands, and their low-pressure shifts. In tandem with the carbonate stretching and bending modes both having lower frequency components that initiate around 63 GPa, each of the new features have anomalously low pressure shifts. Such low-pressure shifts indicate that the C-O bond strengths associated with these carbonate vibrations are almost unchanged in strength between 63 and 86 GPa, despite substantial compaction. These minimal shifts are also compatible with a progressively stronger fourth C-O bond forming, with weakening of the C-O bonds of the carbonate group as the additional oxygen becomes progressively more strongly bound to the unit. Furthermore, Mao et al. (2011) (their Supplemental Info) report a slight change in the lattice parameters of dolomite-III near 63 GPa, indicating that a shift in compressional mechanism occurs near this pressure. This shift is consistent with our interpretation that new C-O bonds begin to form at this pressure.

At our highest pressures, the spectra continue to be most readily explained by a 3+1 coordination environment for a subgroup of the carbonate ions. Notably, carbonate vibrations that have normal frequencies (readily extrapolated from lower-pressure conditions) and pressure shifts continue to dominate the spectra, indicating that a mix of 3+1 coordinated carbonate groups and highly compacted, but three-fold carbonate groups, are present within dolomite-III. This interpretation implicitly requires that these vibrations involve carbon environments that are substantially distorted. Thus, the absolute Raman amplitude of these vibrations is expected to underrepresent the true concentration of the more highly coordinated carbon cations within the crystal, since Raman bands are stronger for more symmetric vibrations and environments (for example, Williams 1995). We believe that it is unlikely that full tetrahedral coordination of carbon is achieved in any of the carbonate units in dolomite-III over this pressure range, since an enhancement in intensity of the bands associated with the weaker C-O bonds would be

anticipated if the local environment became more symmetric; it is also possible that the frequency decrement associated with full tetrahedral coordination might be larger than we observe (Sun et al. 2009) .

Implications

$CaMg(CO_3)_2$ evolves a novel bonding environment of carbon above 63 GPa, as manifested by a subset of weaker C-O bonds being present above this pressure in dolomite-III. These weaker C-O bonds are plausibly generated by an additional oxygen progressively approaching one of the carbonate ions, resulting in a 3+1 coordination of the carbonate group, verifying a prediction by Merlini et al. (2012). The broad diversity of distorted structural environments within both the carbonate groups and cation sites (based on the wide range in frequency spanned by the lattice modes) in the dolomite-III structure, indicate that this is a phase in which incompatible elements are likely to substitute. Thus, as dolomite-III is expected to be a stable phase within oxidized zones in the deep mantle (consistent with its observed thermal stability), the low symmetry/distortion of its cation sites likely render it a major host for incompatible elements in the lower mantle. This conclusion provides a potential mineralogic basis for the affinity between carbonate metasomatism and incompatible element signatures in magmas with deep mantle provenances or long-term mantle residence times (Collerson et al. 2010; Castillo 2015; Weiss et al. 2016). Thus, because of its novel structural characteristics and multiple coordination environments, the high-pressure phase of dolomite may be critical in the incompatible element cycling associated with deeply-derived carbon-bearing magmas.

Typically, an increase in coordination number leads to an increase in entropy (e.g. Navrotsky 1980) which implies that dolomite-III's entropy may increase under pressure ase the 3+1 coordination is generated. Dolomite-Iv, which is characterized by four-coordinate carbon, is

a relatively symmetric structure (although it may have divalent cation disorder (Merlini et al. 2017). The mixed coordination carbon environments and highly distorted carbonate and metal cation sites that we characterize in dolomite-III indicate that this phase is likely to be higher entropy than the symmetric ring structure documented for dolomite-IV synthesized at 120 GPa and 2,500˚C (Merlini et al. 2017). Thus, the transition from the highly disordered structure of dolomite-III to higher symmetry dolomite-IV may produce a situation that is reversed from that of the well-known coordination change and transition from γ-spinel to perovskite (Bina and Helffrich 1994). Thus, on structural grounds, we expect that the Clapeyron slope of the dolomite III-IV transition is likely to be positive. Hence, the high temperatures present near the base of Earth's mantle (Anzellini et al. 2013) may result in dolomite-III being stabilized throughout much of Earth's mantle.

References

Alt, J.C., and Teagle, D.A.H. (1999) The uptake of carbon during alteration of ocean crust. Geochimica et Cosmochimica Acta, 63, 1527–1535.

Anzellini, S., Dewaele, A., Mezouar, M., Loubeyre, P., and Morard, G. (2013) Melting of iron at Earth's inner core boundary based on fast X-ray diffraction. Science, 340, 464–466.

Bina, C.R., and Helffrich, G. (1994) Phase-transition Clapeyron slopes and transition zone seismic discontinuity topography. Journal of Geophysical Research, 99, 15853–15860.

Boulard, E., Gloter, A., Corgne, A., Antonangeli, D., Auzende, A.-L., Perrillat, J.-P., Guyot, F., and Fiquet, G. (2011) New host for carbon in the deep Earth. Proceedings of the National Academy of Sciences, 108, 5184–5187.

Boulard, E., Pan, D., Galli, G., Liu, Z.X., and Mao, W.L. (2015) Tetrahedrally coordinated carbonates in Earth's lower mantle. Nature Communications, 6, 1–5.

253 Castillo, P.R. (2015) The recycling of marine carbonates and sources of HIMU and FOZO ocean
254 island basalts. Lithos, 216–217, 254–263.
255 Cerantola, V., Bykova, E., Kupenko, I., Merlini, M., Ismailova, L., McCammon, C., Bykov, M.,
256 Chumakov, A.I., Petitgirard, S., Kantor, I., and others (2017) Stability of iron-bearing
257 carbonates in the deep Earth's interior. Nature Communications, 8, 15960.
258 Collerson, K.D., Williams, Q., Ewart, A.E., and Murphy, D.T. (2010) Origin of HIMU and EM-1
259 domains sampled by ocean island basalts, kimberlites and carbonatites: The role of CO_2-
260 fluxed lower mantle melting in thermochemical upwellings. Physics of the Earth and
261 Planetary Interiors, 181, 112–131.
262 Corgne, A., and Wood, B.J. (2005) Trace element partitioning and substitution mechanisms in
263 calcium perovskites. Contributions to Mineralogy and Petrology, 149, 85–97.
264 Dasgupta, R., Hirschmann, M.M., and Stalker, K. (2006) Immiscible transition from carbonate-
265 rich to silicate-rich melts in the 3 GPa melting interval of eclogite + CO_2 and genesis of
266 silica-undersaturated ocean island lavas. Journal of Petrology, 47, 647–671.
267 Duba, A.G., and Shankland, T.J. (1982) Free carbon & electrical conductivity in the Earth's
268 mantle. Geophysical Research Letters, 9, 1271–1274.
269 Efthimiopoulos, I., Jahn, S., Kuras, A., Schade, U., and Koch-Müller, M. (2017) Combined high-
270 pressure and high-temperature vibrational studies of dolomite: phase diagram and evidence
271 of a new distorted modification. Physics and Chemistry of Minerals, 0, 1–12.
272 Gillet, P., Biellmann, C., Reynard, B., and McMillan, P. (1993) Raman spectroscopic studies of
273 carbonates Part I: High-pressure and high-temperature behaviour of calcite, magnesite,
274 dolomite and aragonite. Physics and Chemistry of Minerals, 20, 1–18.
275 Hirschmann, M.M., and Dasgupta, R. (2009) The H/C ratios of Earth's near-surface and deep

reservoirs, and consequences for deep Earth volatile cycles. Chemical Geology, 262, 4–16.

Isshiki, M., Irifune, T., Hirose, K., Ono, S., Ohishi, Y., Watanuki, T., Nishibori, E., Takata, M., and Sakata, M. (2004) Stability of magnesite and its high-pressure form in the lowermost mantle. Nature, 427, 60–63.

Koch-Müller, M., Jahn, S., Birkholz, N., Ritter, E., and Schade, U. (2016) Phase transitions in the system $CaCO_3$ at high P and T determined by in situ vibrational spectroscopy in diamond anvil cells and first-principles simulations. Physics and Chemistry of Minerals, 43, 545–561.

Kraft, S., Knittle, E., and Williams, Q. (1991) Carbonate stability in the Earth's mantle: A vibrational spectroscopic study of aragonite and dolomite at high pressures and temperatures. Journal of Geophysical Research, 96, 17997–18009.

Litasov, K.D., Shatskiy, A., Ohtani, E., and Yaxley, G.M. (2013) Solidus of alkaline carbonatite in the deep mantle. Geology, 41, 79–82.

Mao, H.K., Xu, J., and Bell, P.M. (1986) Calibration of the ruby pressure gauge to 800 kbar under quasi-hydrostatic conditions. Journal of Geophysical Research, 91, 4673–4678.

Mao, Z., Armentrout, M., Rainey, E., Manning, C.E., Dera, P., Prakapenka, V.B., and Kavner, A. (2011) Dolomite III : A new candidate lower mantle carbonate. Geophysical Research Letters, 38, 2–5.

Merlini, M., Crichton, W. a, Hanfland, M., Gemmi, M., Müller, H., Kupenko, I., and Dubrovinsky, L. (2012) Structures of dolomite at ultrahigh pressure and their influence on the deep carbon cycle. Proceedings of the National Academy of Sciences, 109, 13509–13514.

Merlini, M., Cerantola, V., Gatta, G.D., Gemmi, M., Hanfland, M., Kupenko, I., Paolo, L.,

Muller, H., and Zhang, L. (2017) Dolomite-IV : Candidate structure for a carbonate in the Earth's lower mantle. American Mineralogist, 102, 1763–1766.

Nakamoto, K. (1986) Infrared and Raman spectra of inorganic and coordination compounds, 4th ed. Wiley-Interscience, New York.

Navrotsky, A. (1980) Lower mantle phase transitions may generally have negative pressure-temperature slopes. Geophysical Research Letters, 7, 709–711.

Nicola, J., Scott, J., Couto, R., and Correa, M. (1976) Raman spectra of dolomite [$CaMg(CO_3)_2$]. Physical Review B, 14, 4676–4678.

Oganov, A.R., Glass, C.W., and Ono, S. (2006) High-pressure phases of $CaCO_3$: Crystal structure prediction and experiment. Earth and Planetary Science Letters, 241, 95–103.

Pilati, T., Demartin, F., and Gramaccioli, C.M. (1998) Lattice-dynamical estimation of atomic displacement parameters in carbonates: Calcite and aragonite $CaCO_3$, dolomite $CaMg(CO_3)_2$ and magnesite $MgCO_3$. Acta Crystallographica Section B Structural Science, 54, 515–523.

Rosenthal, A., Hauri, E.H., and Hirschmann, M.M. (2015) Experimental determination of C, F, and H partitioning between mantle minerals and carbonated basalt, CO_2/Ba and CO_2/Nb systematics of partial melting, and the CO_2 contents of basaltic source regions. Earth and Planetary Science Letters, 412, 77–87.

Santillán, J., and Williams, Q. (2004) A high-pressure infrared and X-ray study of $FeCO_3$ and $MnCO_3$: Comparison with $CaMg(CO_3)_2$-dolomite. Physics of the Earth and Planetary Interiors, 143, 291–304.

Santillán, J., Williams, Q., and Knittle, E. (2003) Dolomite-II: A high-pressure polymorph of $CaMg(CO_3)_2$. Geophysical Research Letters, 30, 1054.

Shcheka, S.S., Wiedenbeck, M., Frost, D.J., and Keppler, H. (2006) Carbon solubility in mantle minerals. Earth and Planetary Science Letters, 245, 730–742.

Steinfink, H., and Sans, F.J. (1959) Refinement of the crystal structure of dolomite. American Mineralogist, 44, 679–682.

Sun, J., Klug, D.D., Martonak, R., Montoya, J.A., Lee, M.S., Scandolo, S., and Tosatti, E. (2009) High-pressure polymeric phases of carbon dioxide. Proceedings of the National Academy of Sciences, 106, 6077–6081.

Weiss, Y., Class, C., Goldstein, S.L., and Hanyu, T. (2016) Key new pieces of the HIMU puzzle from olivines and diamond inclusions. Nature, 537, 666–670.

Wicks, J.K., and Duffy, T.S. (2016) Crystal Structures of Minerals in the Lower Mantle. In Hidenori Terasaki and R.A. Fischer, Eds., Deep Earth: Physics and Chemistry of the Lower Mantle and Core, Geophysical Monograph pp. 69–87. John Wiley & Sons, Inc.

Williams, Q. (1995) Infrared, Raman and Optical Spectroscopy of Earth Materials. In T.J. Ahrens, Ed., Mineral physics and crystallography: A Handbook of Physical Constants pp. 291–302. AGU Press, Washington DC.

Acknowledgements

We would like to thank Earl O'Bannon and Elise Knittle for useful discussions and Simon Teat for help at ALS beamline 11.3.1. This work was supported by the US NSF via EAR-1620423. We would like to thank Andrew Doran and Martin Kunz at the Advanced Light Source and Sergey Tkachev at the Advanced Photon Source for gas loading: this was supported by COMPRES under NSF Cooperative Agreement EAR 11-57758. We would like to thank Dale Burns at Stanford University for assistance with the electron microprobe analysis. We would like to thank three anonymous reviewers for their helpful comments.

Figures

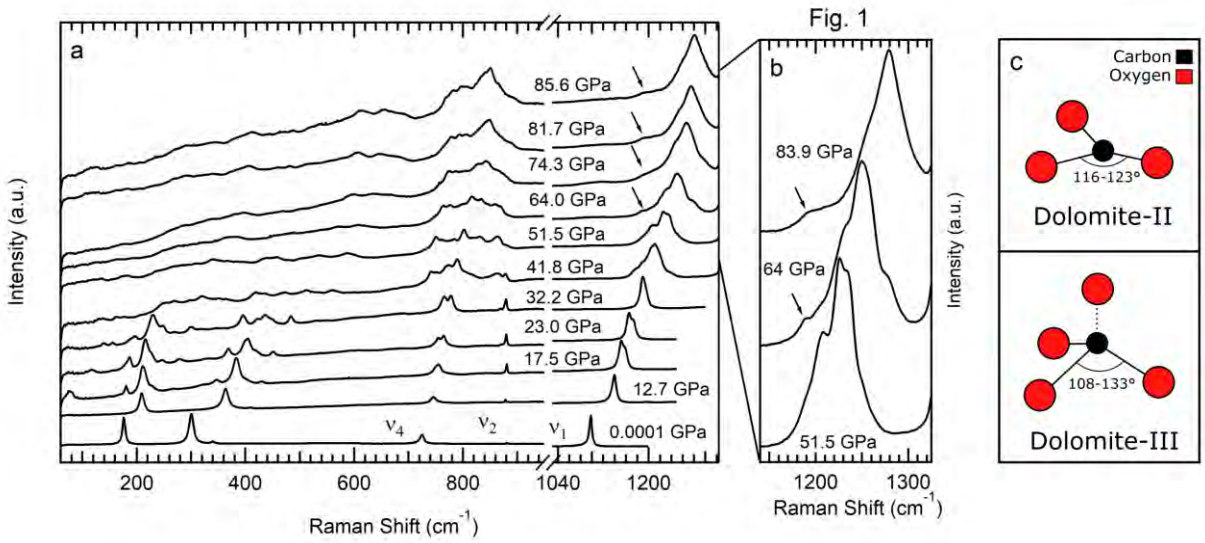

Figure 1. Representative Raman spectra of dolomite under compression at room temperature (spectra are vertically offset for clarity). (**a**) Lattice modes and the carbonate modes associated with the out-of-plane bends, in-plane bends and symmetric stretches are shown. Arrows indicates the peak(s) that is indicative of the onset of 3+1 coordination. Variable relative amplitudes of peaks in some spectra are likely associated with preferred orientation effects. (**b**) An enlarged view of the carbonate's symmetric stretch at 52, 64 and 84 GPa. Again, arrows indicate the peak that is indicative of the onset of 3+1 coordination. (**c**) Schematic depiction of the transition of a 3-fold coordinated carbonate ion in dolomite-II to 3+1 coordinated in dolomite-III.

This is a preprint, the final version is subject to change, of the American Mineralogist (MSA)
Cite as Authors (Year) Title. American Mineralogist, in press.
(DOI will not work until issue is live.) DOI: http://dx.doi.org/10.2138/am-2017-6270

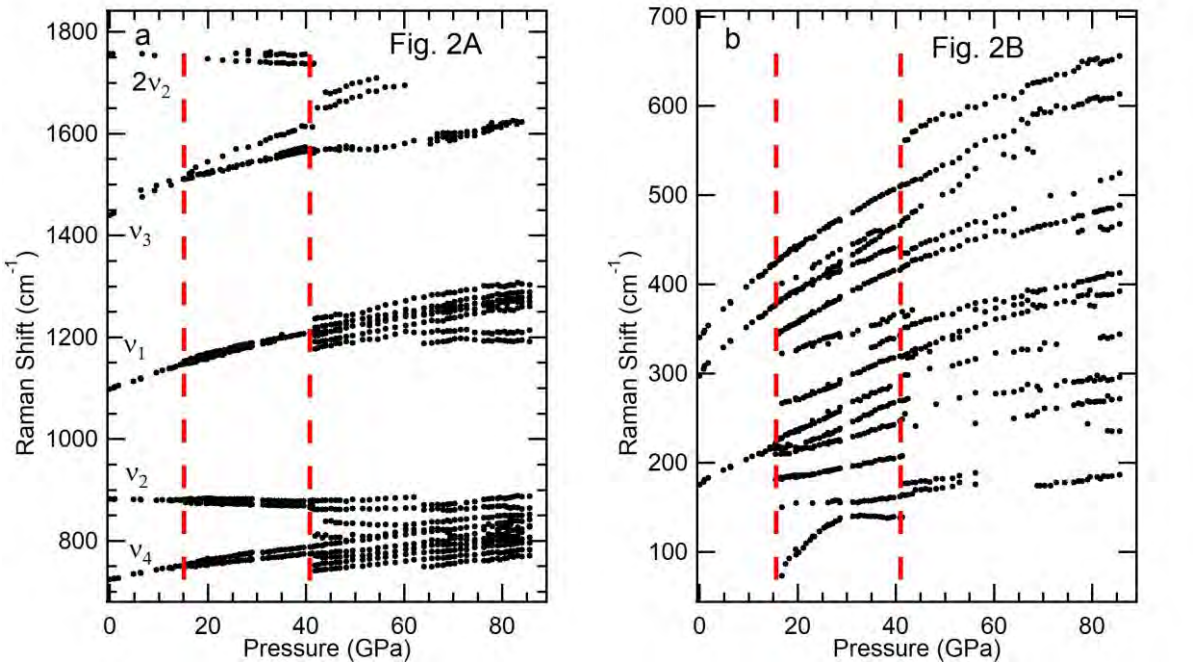

Figure 2. Peak positions of observed Raman modes as a function of pressure. (**a**) Carbonate modes associated with the out-of-plane bend (ν_2), in-plane bend (ν_4), symmetric stretch (ν_1) and asymmetric stretch (ν_3). $2\nu_2$ represents an overtone of the out-of-plane bend. (**b**) Lattice modes of dolomite. These predominantly involve relative motion between the carbonate groups and the divalent cations. Vertical dashed red lines indicate phase transitions.